

THE WIND AND TEMPERATURE STRUCTURE OF NOCTURNAL COLD FRONTS IN THE FIRST 1,420 FEET

KENNETH C. BRUNDIDGE

Texas A and M University, College Station, Texas

ABSTRACT

Results are presented of determinations of the temperature structure and relative streamlines for eleven cold fronts as obtained from data collected on the 1420-ft. TV transmitting tower at Cedar Hill, Tex.

The temperature patterns were found to approximate the textbook case only when the frontal zones were strongly baroclinic and some instances of extreme overrunning were found when a pre-frontal nocturnal inversion existed. The relative flow patterns generally show a confluence of warm and cold air within the frontal zone, implying that the front cannot be treated as a substantial surface. Vertical turbulent mixing appears to be an important factor in the maintenance of the temperature structure.

1. INTRODUCTION

In 1960 the Air Force Cambridge Research Laboratories established a facility which has come to be called the Dallas or Cedar Hill tower [15]. The facility was actually the WFAA-KRLD TV transmitting tower, located about 20 mi. southwest of Dallas, which was instrumented to measure wind and temperature at 12 levels from 30 ft. to 1,420 ft. above the ground. Details of the structure and instrumentation performance are provided by Mitchem and Jehn [9].

The data from the tower were intended primarily for investigations of the low-level jet [4, 7, 8]. However, it was apparent that the data were suitable for other types of studies as well and have been so utilized [5, 16, 17].

In the present instance, the data have been used to determine the mesoscale structure of 11 cold fronts which passed the tower during the fall and winter months of 1961-62. While texts such as Saucier [14], provide considerable information on the characteristics and structure of fronts, the conclusions mainly are based on accumulated experience in working with synoptic-scale observations. In view of the relatively great spacing of observing stations on this scale, little is known of a detailed nature about the temperature structure and relative wind flow at points above the ground in frontal zones. The closest approach to the scale of observations provided by the Cedar Hill tower has been in the work of the Thunderstorm Project [10], and that of Clarke [2]. In both instances, however, data were obtained by frequent raob and pilot balloon releases.

2. ANALYSIS TECHNIQUES

The tower data provide time cross sections at a fixed point. However, with suitable assumptions a conversion

can be made to space cross sections, as has been done by Clarke [2]. For this purpose consider a right-handed coordinate system with the positive x axis directed normal to and in the direction of motion of the front at the ground. If the speed of the front is c and D/Dt represents the local change with time at a point fixed relative to the moving front, then

$$\frac{D}{Dt} = \frac{\partial}{\partial t} + c \frac{\partial}{\partial x},$$

or

$$\frac{\partial}{\partial x} = \frac{\partial}{\partial X} + \frac{1}{c} \frac{D}{Dt}, \quad (1)$$

where $\delta X = -c \delta t$. If the air is assumed to be incompressible, then the continuity equation and equation (1) lead to

$$w = - \int_0^z \left(\frac{\partial u}{\partial X} + \frac{\partial v}{\partial y} + \frac{1}{c} \frac{Dw}{Dt} \right) dz \quad (2)$$

As discussed by Clarke [2] and Beniura [1], the second and third terms are generally negligible in comparison with the first term in the integrand of equation (2). The smallness of the third term will also be indicated by the comparisons shown in table 3. From equation (1) the time cross sections for u may then be treated as space cross sections.

The velocity components in the plane of the cross section may be expressed in terms of a relative stream function, ψ , such that

$$w = - \frac{\partial \psi}{\partial X}, \quad u - c = \frac{\partial \psi}{\partial z}, \quad (3)$$

and

$$\psi = \int_0^z (u - c) dz, \quad (4)$$

where ψ is assumed to be zero at the ground.

It is evident from this procedure that the computed

relative flow is very much dependent upon the orientation and speed of the front. Several methods were used for this determination. Hourly sectional maps were plotted and analyzed for each case to obtain one estimate. A second estimate was obtained for those cases in which weather stations in the area reported frontal passage times which could be used in conjunction with the tower passage time to determine isochrones of position. Finally, in some instances temperature and wind data were available from a group of eight 55-ft. towers surrounding the main tower. Lines connecting these towers roughly formed a box about 7 mi. on a side with the main tower lying on the NW-SE diagonal. A small-scale terrain map of the region showing the positions of all the towers is given by Clayton [3]. These data provided a very accurate check on the speed and orientation of the front. It should be mentioned here that the fronts were located on the hourly maps so as to give the best possible agreement between the pressure, wind, and temperature fields. Continuity was carefully observed. An examination of these analyses was made in relation to the reported times of frontal passage. From this it appeared that the main criterion being utilized by the weather station observers to report passage times was the advent of the wind shift. Therefore, the time of the wind shift at the various towers was used in determining the movement of the front. In all but 3 of the 11 cases there were at least two checks on the orientation and speed of the front. The results of these determinations are given in table 1.

In those instances when a barograph trace at the base of the tower was available, the reported tower temperatures were converted to potential temperatures. This was accomplished through use of the hydrostatic and Poisson relations, as described by Wong [1]. However, the pressures used in the computations were uncorrected and in some cases differed from the value which would be expected on the basis of synoptic analysis by as much as 10 mb. Consequently, the computed potential temperature values are somewhat in error; however, the error should be uniform over the several hours of data under consideration in each case and thus the potential temperature patterns should be correct. The necessity of assigning the observed pressure to the 30-ft. level of the tower also contributed some error.

One final point should be mentioned. The tower data were reported at 10-min. intervals and represented averages over all but the last 20 sec. of the preceding 10-min. period. Thus, features in the wind or temperature fields moving with the front and having wavelengths of less than the equivalent of 20 min. of travel time of the frontal system would not be distinguished. Furthermore, the amplitude of observable features would be somewhat damped and their apparent time of occurrence would tend to lag their true time of occurrence by up to 10 min. From the frontal speeds given in table 1, the tower was, on the average, capable of detecting mesoscale features with wavelengths of about 7 mi. or greater.

TABLE 1.—Frontal speeds and orientations. *MLW*=Mineral Wells, Tex.; *ACF*=Amon Carter Field, Fort Worth, Tex.; *FTW*=Fort Worth (Meacham), Tex.; *DAL*=Dallas, Tex.

Case	Direction from which moving (deg.) and speed (mi. hr. ⁻¹)	Basis for determination
1.....	325, 20	Hourly maps; reported passage times at MWL, FTW, DAL, and tower.
2.....	347, 11.3	Hourly maps; reported passage times at ACF, FTW, and tower.
3.....	330, 17	Hourly maps; normal wind components at middle levels of tower.
4.....	307, 12.5	Hourly maps; reported passage times at ACF, DAL, and tower.
5.....	342, 9	Hourly maps; reported passage times at ACF, DAL, and tower; small and main tower data.
6.....	311, 28.3	Hourly maps; small and main tower data.
7.....	304, 34.5	Hourly maps.
8.....	312, 30	Hourly maps.
9.....	333, 13	Hourly maps.
10.....	315, 15	Hourly maps; small and main tower data.
11.....	345, 22	Hourly maps; small and main tower data.

3. RESULTS

The cases are presented in chronological order in figures 1 through 23.¹ In each case, the fields of temperature and relative streamlines are provided. In some instances, figures are also given of a sectional surface map close in time to the frontal passage time at the tower, along with a raob cross section. In view of the large number of cases, only the major features will be discussed at this point. Details will be brought up for several cases in the next section. In examining the tower cross sections it should be kept in mind that in terms of the time-space conversion, the horizontal scales differ from one case to another.

Purely by coincidence, all of the cases except Case 8 were nighttime or early morning passages. Consequently, the temperature fields for all cases but Case 8 (fig. 14) show a nocturnal inversion preceding the front for a depth of several hundred feet. The frontal passage time for Case 6 occurred at 2000 CST and the inversion may be seen in figure 11 to have formed at the ground over the preceding 3-hr. period. In each such case the isentropes or isotherms bend at the front and blend into the temperature structure of the frontal zone. This condition made it difficult to determine the true position of the frontal surface. The criterion used in the figures was to place the frontal surface along the line denoting a sharp increase in horizontal temperature gradient which occurred in a consistent manner at all levels of the tower.

Except for Case 9 (fig. 15), it is seen that the frontal surfaces are nearly vertical or tend to tilt forward somewhat. This is particularly true in Cases 6 and 7 (figs. 11 and 12), in which the protrusion amounts to 20 mi. and 50 mi., respectively, over the depth of the tower. Thus, the conditions are very similar to those shown schematically by Saucier [14] in his figures 6.23 (d) and (e), if these are considered in combination. Because there is an inversion associated with the "overrunning"

¹ Cases 9, 10, and 11 (figs. 15-23) are taken from an incomplete Master of Science thesis by D. S. Shimomura, Texas A & M University.

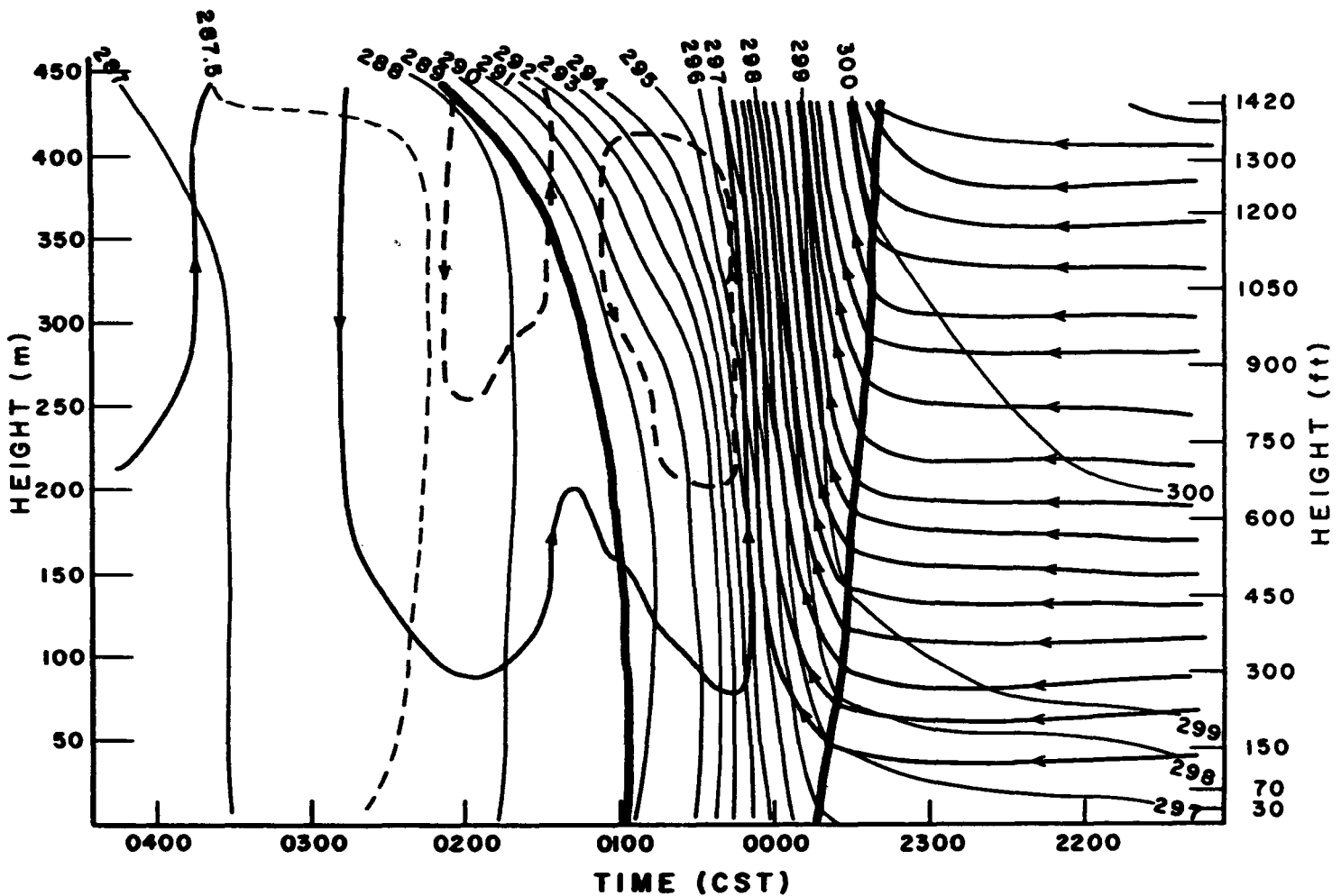


FIGURE 1.—Time cross section of the smoothed fields of potential temperature at 1° K. increments and relative streamlines for Case 1, September 24–25, 1961. Heavy, solid lines represent the boundaries of the frontal zone.

cold front, the temperature distribution along a vertical from the ground up into the protrusion is actually stable and the inverted front is maintained.

It should also be noted, except for Cases 1, 9, 10, and 11 (figs. 1, 15, 18, and 21) in which the baroclinity of the frontal zone is particularly large, that a trailing side of the frontal zone is not always clearly defined and hence has not been indicated in the figures. Furthermore, the temperature structure may take on a variety of shapes, appearing to depend to some extent upon the degree of baroclinity. For example, in Cases 1, 9, 10, and 11 the frontal zones are of fairly constant thickness for about the first 500 ft. above the ground but broaden out quite rapidly, by a factor of three to five, near the top of the tower. Cases 3 and 4 (figs. 5 and 7) are also fairly baroclinic but involve double concentrations of isotherms. For the somewhat weaker field of Case 8 (fig. 14), the frontal zone appears to be of about constant thickness over the depth of the tower. The other cases essentially defy description, although Cases 2 and 5 (figs. 3 and 9)

show some measure of similarity for about the first 3 hr. after frontal passage.

Generally, the criterion used for locating the frontal surface provided good agreement with the wind-shift line at the ground; however, as seen for Case 4 in figure 7, the wind-shift line then fell behind the frontal surface at the upper levels. Furthermore, the line along which the component of the wind parallel to the front changed sign, i.e., the line of $v=0$, was found to lag behind the wind-shift line. Here, wind-shift is meant as a significant veering of the wind over a 10-min. period. In the cases examined here, the wind direction change at 30 ft. was never less than 19° and in Case 1 was as much as 143°. Smaller values, but generally exceeding 10°, were found at the upper levels of the tower.

In Case 2 (fig. 3) and in all but a small region of Case 7 (fig. 12) the relative motion was found everywhere to be from warm to cold. Otherwise, the relative streamlines show a general tendency for confluence to occur somewhere behind the frontal surface. The warm-air current

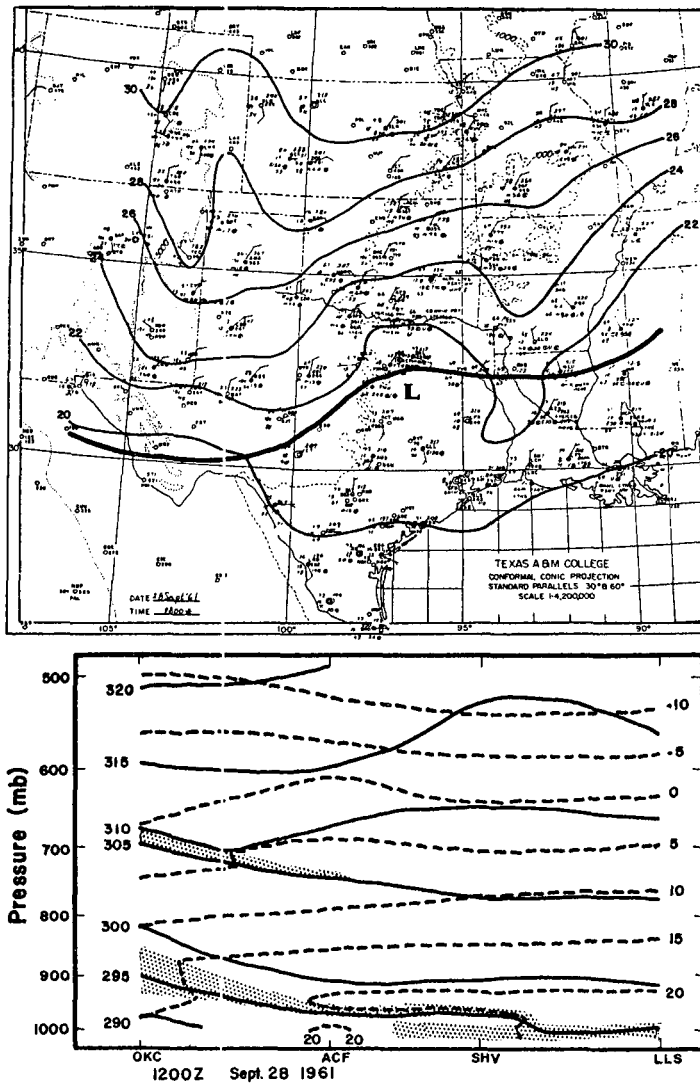


FIGURE 2.—Sectional surface map and cross section for Case 2, September 28, 1961. The heavy, solid line gives the surface position of the front, isobars are at 2-mb. intervals. In the cross section the solid lines are isentropes ($^{\circ}\text{K}$.), dashed lines are isotherms ($^{\circ}\text{C}$.), and the stippled areas represent the front and stable layers.

fairly well parallels the isentropic surfaces in the frontal zone and over a depth of several hundred feet in the warm air ahead of the front. However, the cold-air currents generally cross isentropes and frequently exhibit vortical motion. The latter motion is a reflection of the alternating zones of convergence and divergence which exist in the cold air. It thus appears that the air for some distance into the frontal zone is actually composed of warm air which has been overtaken and cooled semi-adiabatically as it rises in the zone of horizontal convergence found in this region. The question then arises as to whether the temperature field in the cold-air current is constantly changing, or whether the moving air particles

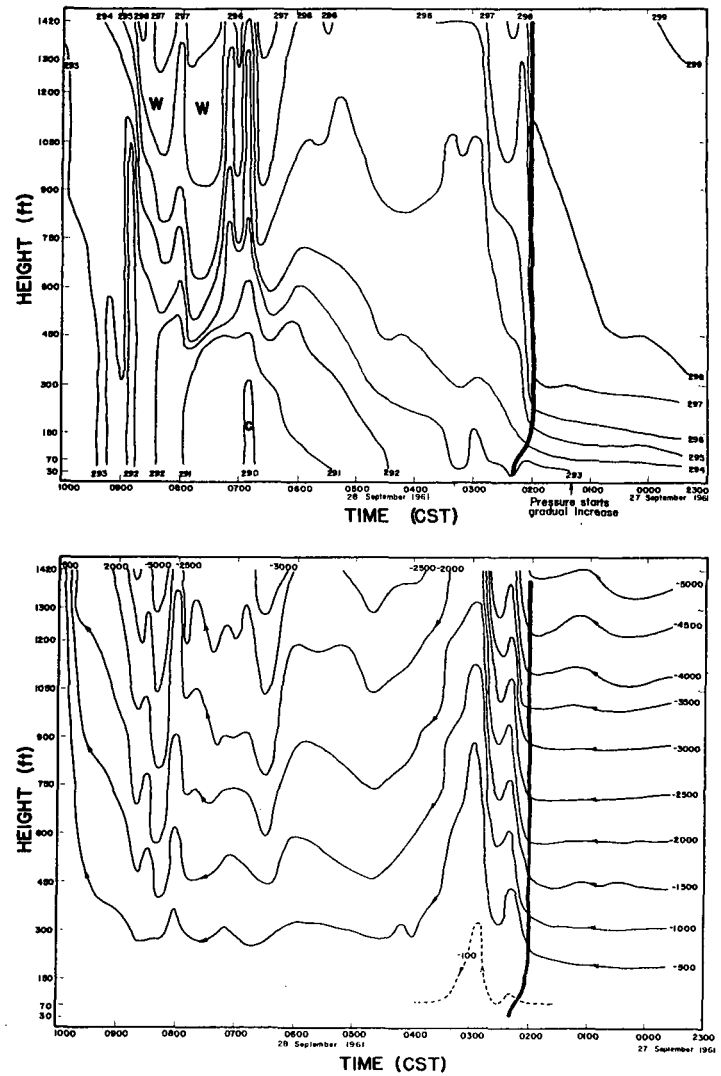


FIGURE 3.—The time cross sections of potential temperature and ψ ($\text{m}^2\text{sec}^{-1}$) as determined at the tower for Case 2. The heavy, solid line represents the front. The direction of the relative motion is indicated by the arrow heads on the ψ lines.

change their temperature in correspondence with the existing field, perhaps by a turbulent flux process with some slight influence by frictional energy conversion.

The influence of friction near the ground may be noted in the relative streamline patterns. It is seen that even when there is a confluence of relative streamlines from the warm- and cold-air sides of the frontal boundary, there is always a shallow layer of air near the ground which is being left behind by the frontal system. This layer is in part made up of an influx of air from the warm side of the frontal boundary and in part from air which feeds down from above in the colder air mass. In order to avoid an extreme number of lines in the diagrams over a

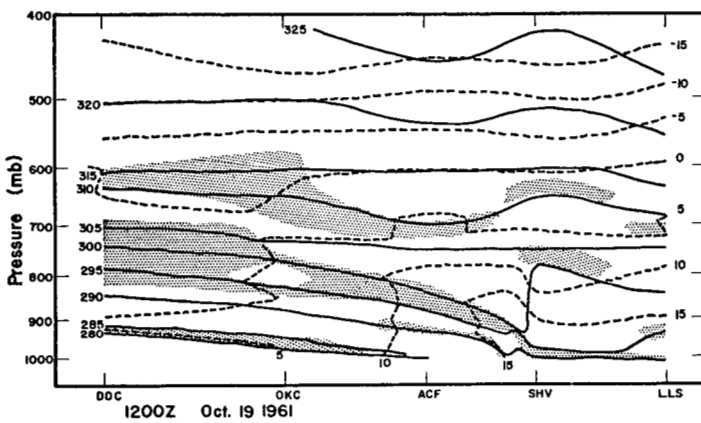
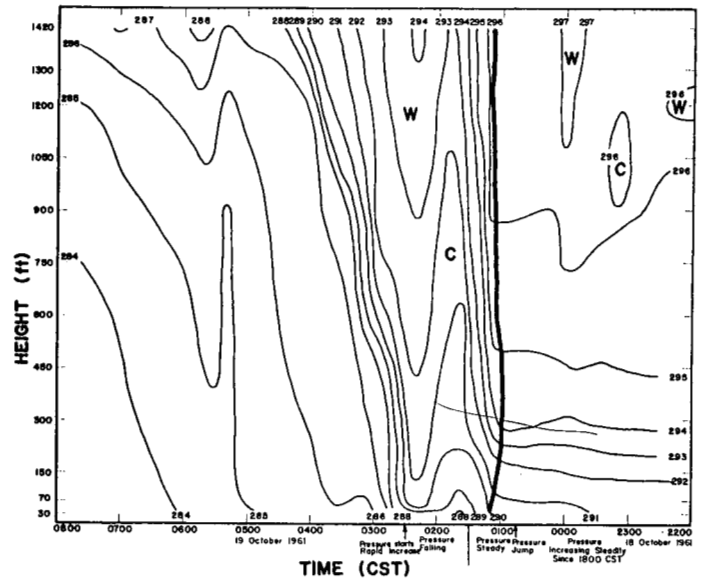
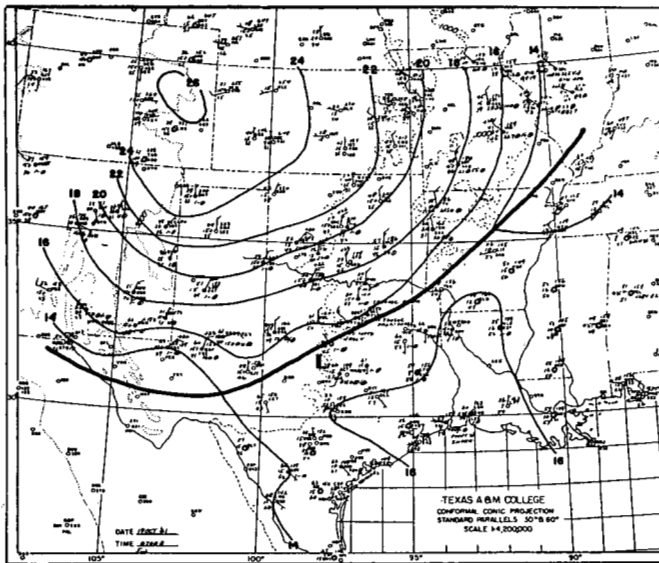


FIGURE 4.—Sectional surface map and cross section for Case 3, October 19, 1961. Legend as described for figure 2.

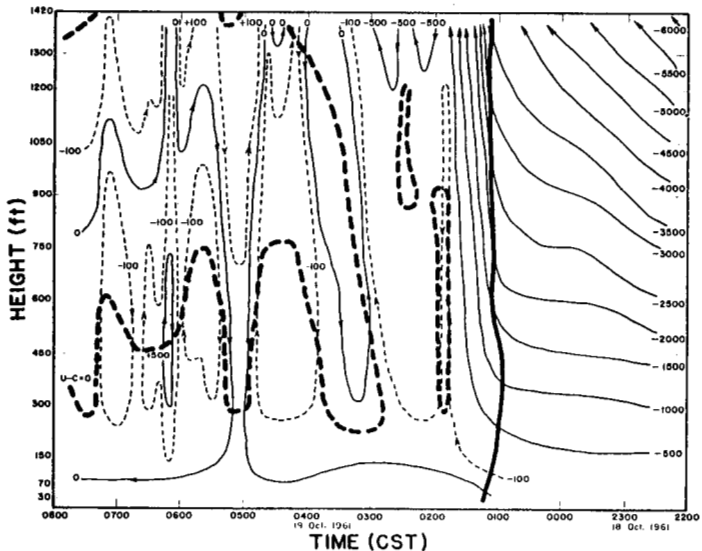


FIGURE 5.—The time cross sections of potential temperature and ψ ($m^2 \text{sec}^{-1}$) at the tower for Case 3. See legend for figure 3. The heavy, dashed lines in the ψ field denote surfaces of $u-c=0$.

small vertical distance, not all of the streamlines necessary to verify this feature are shown. However, it would be useful to recall that the earth's surface is itself a relative streamline directed from the warm to cold side of the frontal zone. This feature may be partially the result of the influence on the wind measurements at the lowest levels of a low building standing approximately 100 ft. to the northwest of the tower. However, it seems likely that the major influence is general surface friction.

A heavy, dashed line labelled $u-c=0$ in the streamline patterns for some of the cases (figs. 5, 7, 9, 11, 12, and 14) marks the separation between air moving faster than the front and that moving slower. There is some indication that the mean height of this surface above the ground is proportional to the speed of the front. At any rate, it is seen that the use of the component of the wind normal to the front determined from a surface wind measurement behind the front as an aid in determining frontal speed

would generally give a deficient speed. From the cases given here, the frontal speed is about double the normal component measured at 30 ft. in the period 20–30 min. after frontal passage. This again bears on the question of what is happening to the temperature field with time. If we assume that parcels conserve their potential temperature as one extreme possibility, then, as a result of the indicated relative motion near the ground, we should expect that super-adiabatic layers should have been found along the ground behind the front. That such layers were not found (except see fig. 1) then directs one to the other extreme, that the potential temperature field moves along relatively unchanged at the speed of the front while the fluid particles change their potential temperatures as they cross isentropes.

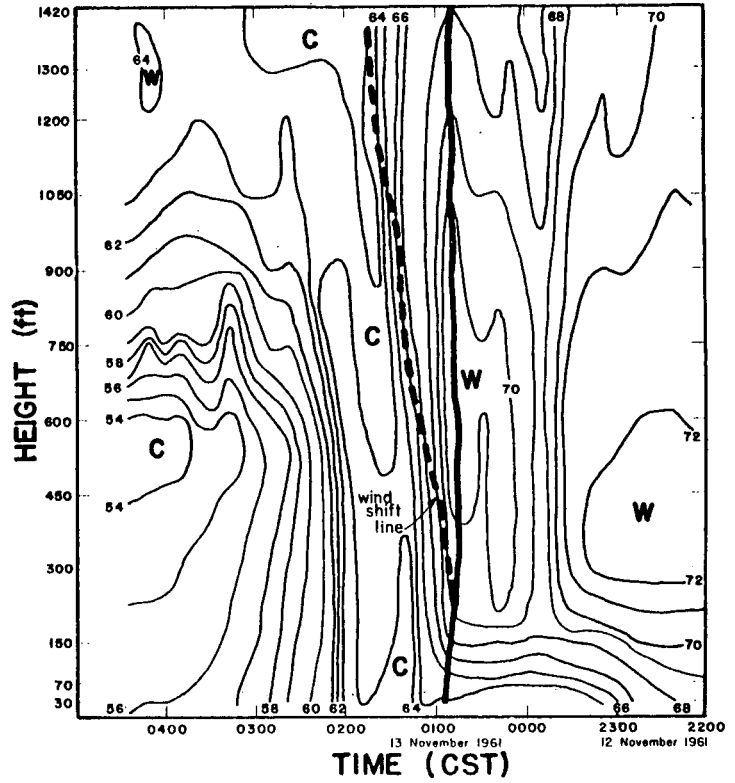
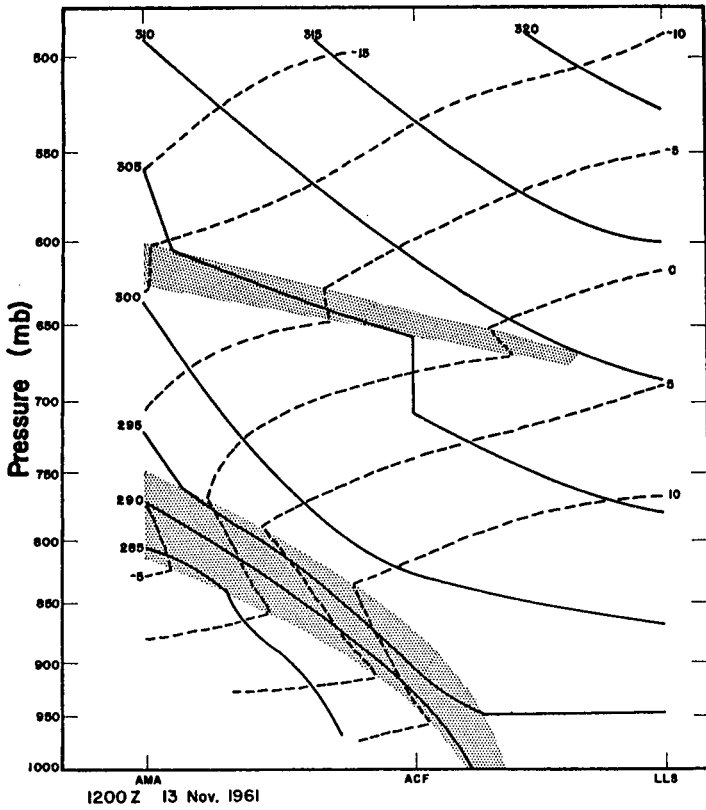


FIGURE 6.—Raob cross section for Case 4, November 13, 1961. See legend for figure 2.

A region of large horizontal convergence was always found near the frontal surface. Consequently, large values of upward motion were computed at the top of the tower in these regions as may be seen from the upward trend and close spacing of the ψ lines in this region. The level of maximum horizontal convergence was always found to lie at some point above the ground. A summary is presented in table 2 for the first eight cases. The table gives the values of the maximum vertical motion and the time of occurrence, the average horizontal convergence in the column at that time, and the level in the column at which the convergence was a maximum. For Case 8, the maximum vertical motion was downward. As might be anticipated, the average convergence was one to two orders of magnitude larger than generally computed on the macroscale, with a corresponding amplification of the vertical motion.

4. ADDITIONAL DETAILS

Case 1 (fig. 1).—This was a relatively strong front for so early in the season in Texas with a temperature drop of 17° F. at 30 ft. and 23.5° F. at 1420 ft. over the 4-hr. period after frontal passage. Most of this temperature change occurred during the first hour. It was also very active some 100 to 150 mi. behind the front, with broken to overcast decks of clouds reported at 2500 to 5000 ft. and thundershower activity west of Mineral Wells, Tex.

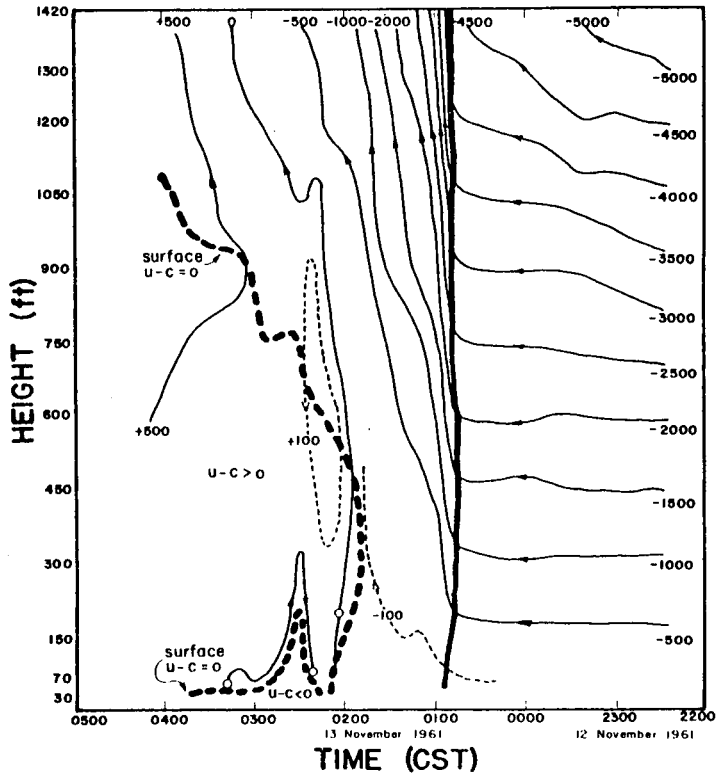


FIGURE 7.—Temperature field (°F.) and ψ ($m.^2sec.^{-1}$) at the tower for Case 4. The heavy, dashed line in the temperature cross section shows the wind shift line while a similar line in the ψ field shows the surface of $u-c=0$.

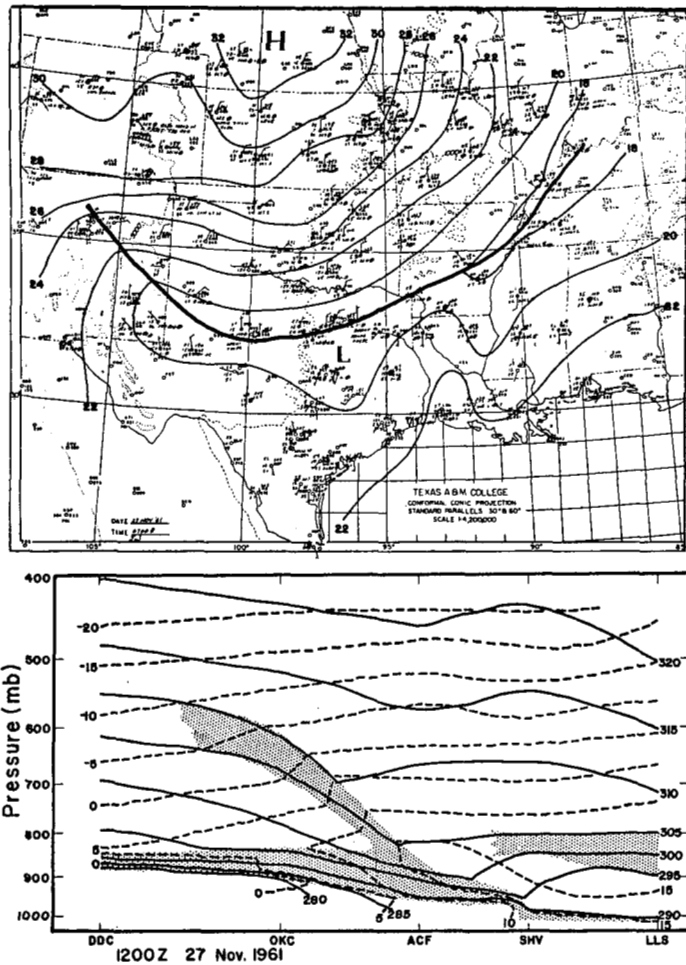


FIGURE 8.—The surface sectional map and cross section for Case 5, November 27, 1961. See legend for figure 2.

(MLW) and in Oklahoma. It is seen in table 2 that the strongest upward motion occurred with this front. Furthermore, the 0600 GMT and 1200 GMT rawin reports at Amon Carter Field, Fort Worth (ACF) indicate that relative motion was directed back along the front for a considerable depth of the atmosphere.

Case 2 (figs. 2 and 3).—This was the weakest front in the study, and because of its poor definition the events associated with it were difficult to interpret.

The synoptic analyses show the front moved only a short distance southeast of the tower and then became diffuse. The raob cross section (fig. 2) shows that the cold air was quite shallow. Shower and thunderstorm activity which had broken out in Oklahoma and western Arkansas followed the southward movement of the front but did not reach Dallas.

It is noted that the relative streamlines (fig. 3) indicate warm-air transport through the front at all levels and times, which might well be indicative that frontolysis was taking place. The ACF 0600 GMT and 1200 GMT rawins also show negative relative motion above the frontal surface. In most of the cases, the front was found to be

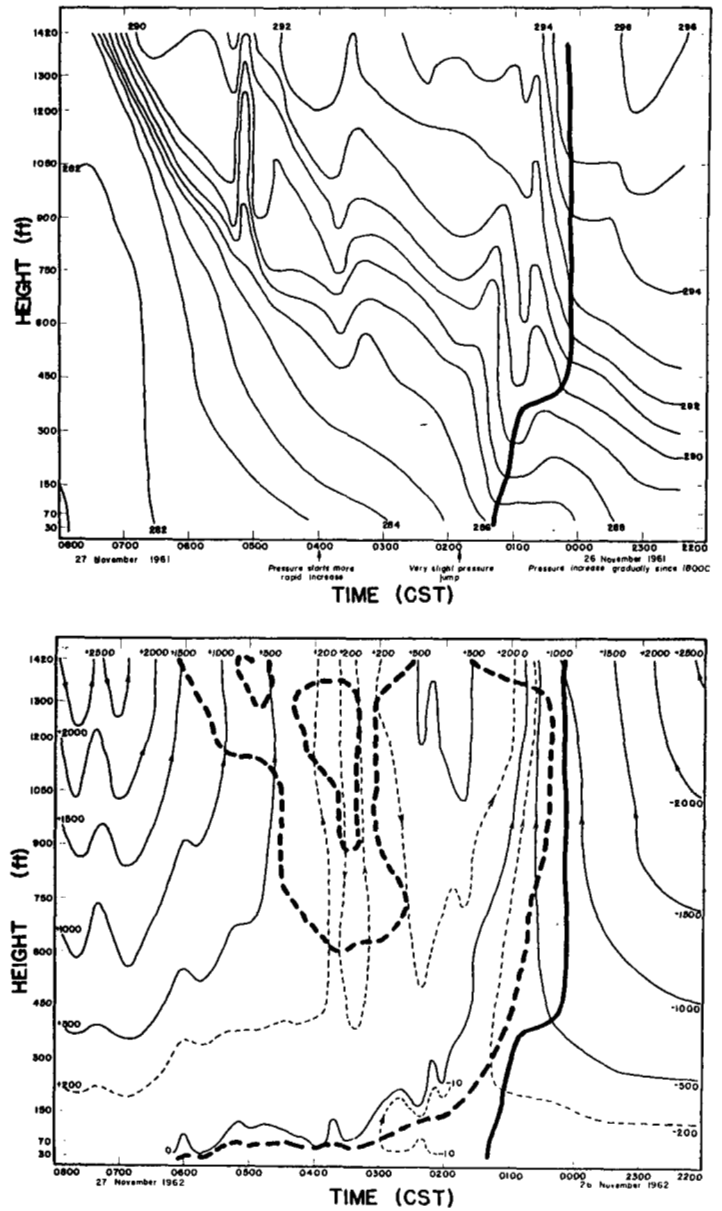


FIGURE 9.—Time cross sections at the tower of potential temperature and ψ ($m^2 \text{sec}^{-2}$) for Case 5. The surfaces of $u-c=0$ are shown as heavy, dashed lines in the ψ field.

moving with a speed equal to the normal component of the wind behind the front at a height of about 600 ft. This was not true of the present case. The tower winds show that except for a small area directly behind the front, the wind was directed toward the colder air. This small area extended up to 800 ft. and was confined to the time interval 0215 to 0345 CST. The average normal component in this region was only about 5.5 mi. hr.⁻¹.

It seems most unlikely that the relative streamlines in figure 3 are completely correct after about 0500 CST because of the uncertainty of the frontal movement after this time. The chaotic appearance of the temperature field after 0600 CST may represent residual effects of the

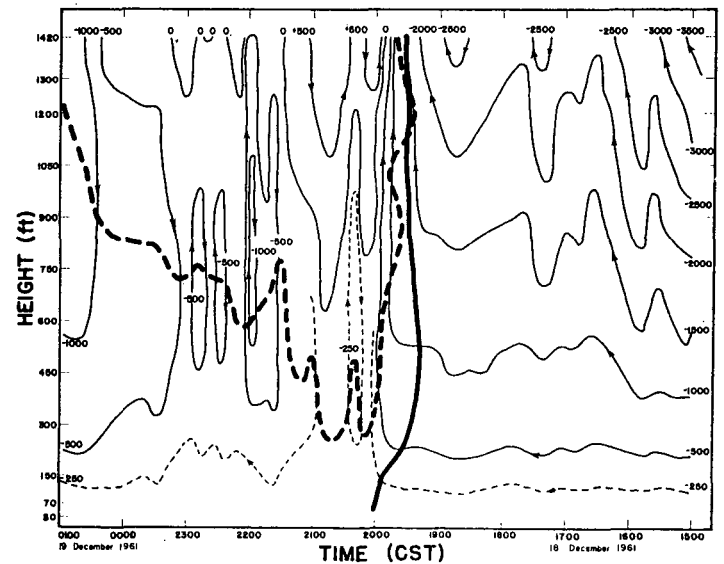
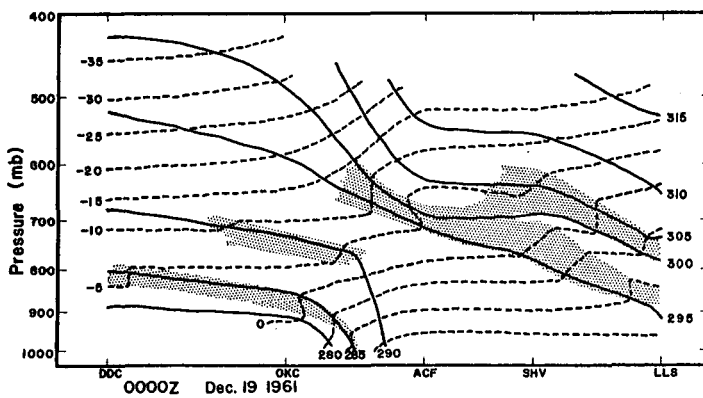
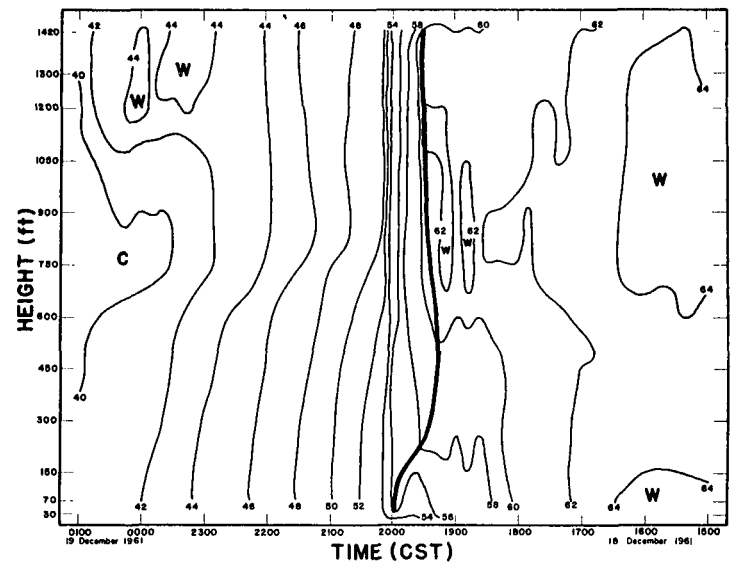
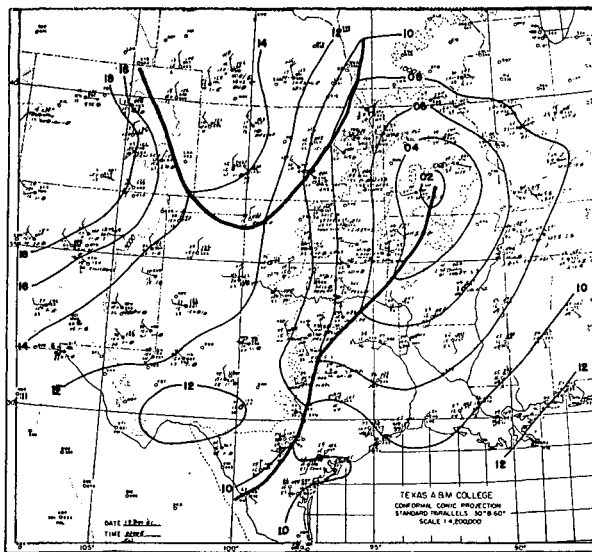


FIGURE 10.—Sectional surface map and cross section for Case 6, December 19, 1961. See legend for figure 2.

FIGURE 11.—Time cross sections at the tower of temperature ($^{\circ}\text{F}$) and ψ ($\text{m}^2\text{sec}^{-1}$) for Case 6. The surface of $u-c=0$ appears as the heavy, dashed line in the ψ field.

thunderstorm activity mentioned previously but more likely indicates the influence of convection after sunrise, such as is observed to occur in the tower records under fair-weather conditions. The winds were variable throughout this period until about 1000 cst when they freshened and swung sharply around from the north, and were accompanied by lower temperatures. This lasted until 1130 cst when the wind veered into the southeast and the temperature increased about 10°F . at the upper levels and about 5°F . near the ground. An hour later, colder air again moved southward.

Case 3 (figs. 4 and 5).—The direction and speed of movement for this case could be determined from the special reports at Waco (ACT), San Angelo (SJT), Perrin Air Field (PNX), MWL, ACF, Dallas (DAL), and the tower. However, various combinations of these reports led to a range of directions from 323° to 343° and a range of speeds from 21 to 43 mi. hr.^{-1} . From the map analyses it was seen that the portion of the front to the west of the tower

site had a different orientation than that portion to the north and was moving at a slower rate. All things considered, it appeared that the bend in the front was being eliminated as the front approached the tower and that a deceleration to a speed of about 20 mi. hr.^{-1} occurred just north of the tower site. It was found that the normal wind speed behind the front at the middle levels of the tower was about 17 mi. hr.^{-1} . Since this was in agreement with the synoptic analyses, this value was used for the computations. A best estimate of the orientation of the front at the time of passage at the tower gave a movement from 330° . This was the only case in which such liberties were taken, but the resulting relative streamlines must be somewhat suspect.

An interesting feature in this case is the second concentration of isotherms which passed the tower starting about 0220 CST (fig. 5). The raob at ACF for 1200 GMT (corresponding time at the tower was 0700 CST) shows two separate stable layers. The potential temperature (θ) values in the upper one corresponded to those found in the first concentration of θ 's to pass the tower. This stable layer contained a sharp increase of moisture with height. The θ 's in the lower layer corresponded to those in the second concentration passing through the tower; however, there was a drop of mixing ratio with height below this layer and a very sharp drop through the layer. It therefore had all the appearances of a subsidence inversion at this level, which was about 2,200 ft. above the ground. The two layers have been analyzed as separate entities in the raob cross section (fig. 4) although the tower data indicate they may have formed a single baroclinic zone at the ground. A difficulty in interpretation that arises here is that the relative streamlines (fig. 5) indicate an influx of moist air through the frontal boundary and then up along both concentrations of potential temperature. This relative motion, at least the horizontal portion of it, is quite well borne out by the ACF rawin at 1200 GMT. Therefore, to the extent that they are correct, it would appear that the warm-air streamlines must wind back into the first concentration of isotherms at levels above the tower top.

Case 4 (figs. 6 and 7).—It is seen in figure 7 that the temperature distribution is quite similar to the previous case in that there was an initial zone of strong horizontal temperature gradient followed about 45 min. later by a second concentration of isotherms. Also, as in the previous case, the surface of $u-c=0$ was associated with this second concentration of isotherms. However, there was no indication of two stable layers in the 1200 GMT ACF sounding (fig. 6) as in the previous case.

Case 7 (fig. 12).—It is unfortunate that there was no way to double check the frontal speed for this case since the relative streamlines look suspicious. That is, as pointed out previously, in the majority of the cases there was good correspondence between the speed of the front and normal wind components behind the front at heights above 300 ft. In the present instance, aside from a very small region above 450 ft. and lying directly above the intersection of the front at the ground in which the normal wind component slightly exceeded 30 mi. hr.⁻¹, the normal wind values above 300 ft. ran closer to 20 mi. hr.⁻¹. Had the latter value been used, the relative motion below 150 ft. would have remained negative, i.e., from warm to cold. However, above 150 ft. and at times after 0730 CST, the flow would have been positive. Thus a line of confluence would have occurred at about 0730 CST. This flow pattern would have been more in keeping with the majority of the other cases but, of course, this does not guarantee its validity.

Cases 9, 10, and 11 (figs. 15-23).—As noted previously these cases, which are instances of a front-squall line

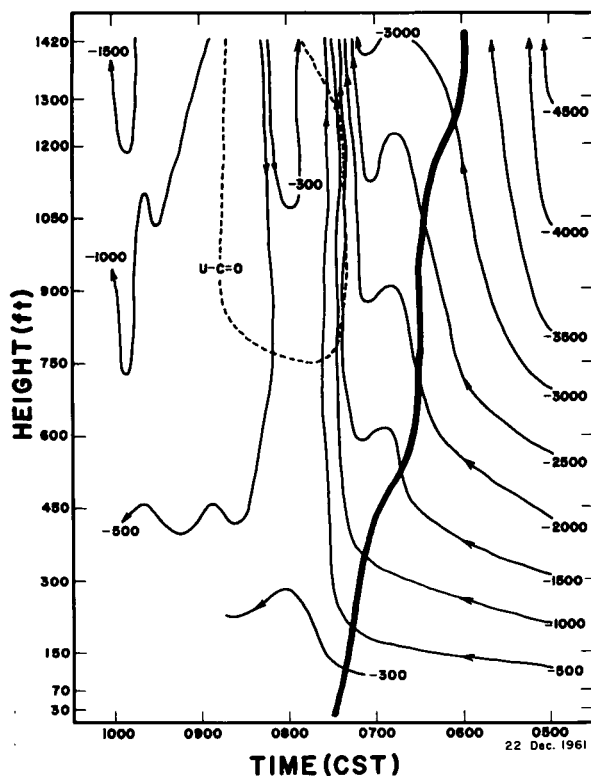
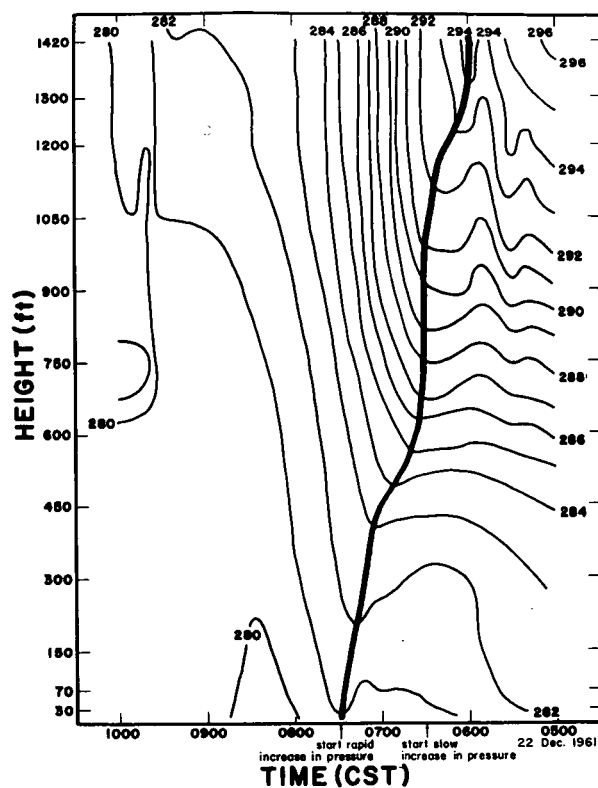


FIGURE 12.—Time cross sections of potential temperature and ψ (m.²sec.⁻¹) for Case 7. The heavy, solid line represents the front. The dashed line in the ψ field gives the surface of $u-c=0$.

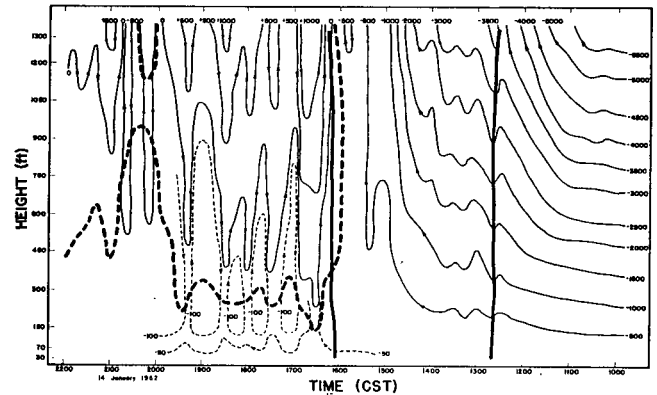
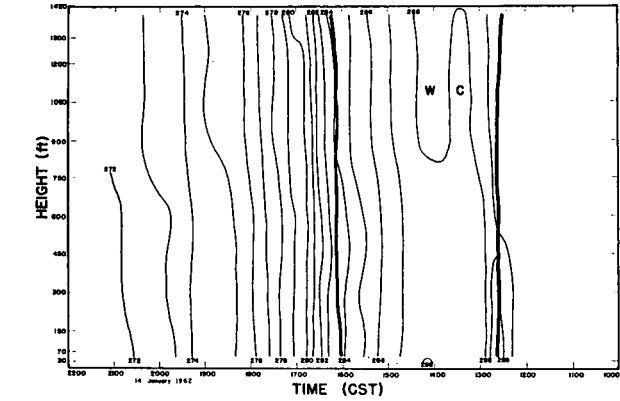
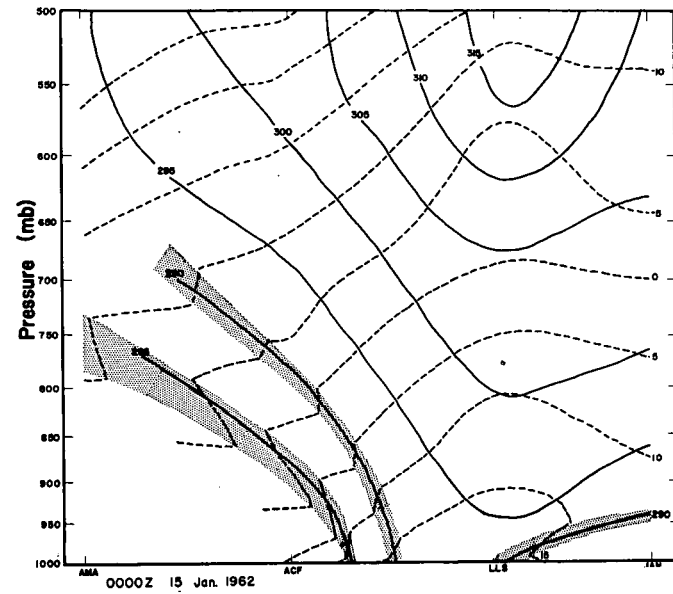
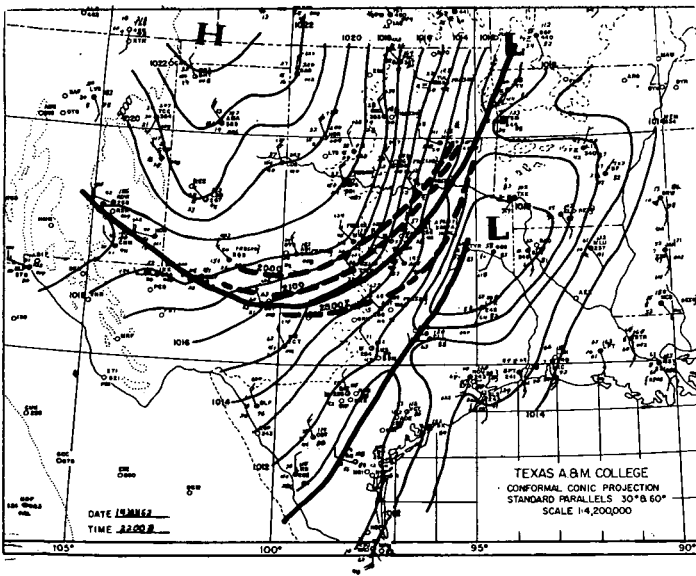


FIGURE 14.—Tower time sections of potential temperature and ψ ($m.^2sec.^{-1}$) for Case 8. ψ field is based on movement of second front (heavy, solid lines) to pass tower and is not representative for the first front. Surface of $u-c=0$ is a heavy, dashed line.

FIGURE 13.—Sectional surface map and cross section for Case 8, January 14, 1962. Heavy, dashed lines on the sectional map show front positions at 1-hr. increments of time.

complex, have been under study by Shimomura. Consequently, only certain prominent features will be remarked upon.

The squall lines are indicated in the figures by vertical dash-dot lines. In Cases 10 and 11 the squall line had

a different orientation and speed than the front. At times prior to the breaks shown in the streamline patterns of figures 19 and 22, the patterns are based upon the squall line movement. At times after the break the streamlines are based upon the movement of the front. In these figures and figure 16 the magnitudes of w , computed for the top of the tower in regions of significant upward or downward motion, are shown along the top. For Case 9 (fig. 16) the horizontal extent of the zone of upward motion preceding the squall line is about 10 mi., whereas for Cases 10 and 11 (figs. 19 and 22), it is closer to 20 mi.

Figures 17, 20, and 23 show the winds measured at the tower at half-hour intervals, except in the vicinity of the squall lines or portions of the frontal zones where they appear at 10-min. increments. North is located at the

TABLE 2.—Vertical motion and divergence

Case	1	2	3	4	5	6	7	8		
Time and magnitude of maximum w [cm. sec. ⁻¹]	2354C, 106	0214C, 40	0254C, 62	0114C, 28	0054C, 36	0034C, 21	0724C, 22	1954C, 16	0724C, 11	1654C, -14
$\nabla \cdot \bar{V}$ [10^{-4} sec. ⁻¹]	-24	-8.9	-13.8	-6.7	-9.4	-4.7	-5.4	-3.7	-2.5	3.2
Level of $\nabla \cdot \bar{V}_{max}$ [ft.]	900	450	1050	300	150	1200	1050	600	750	450

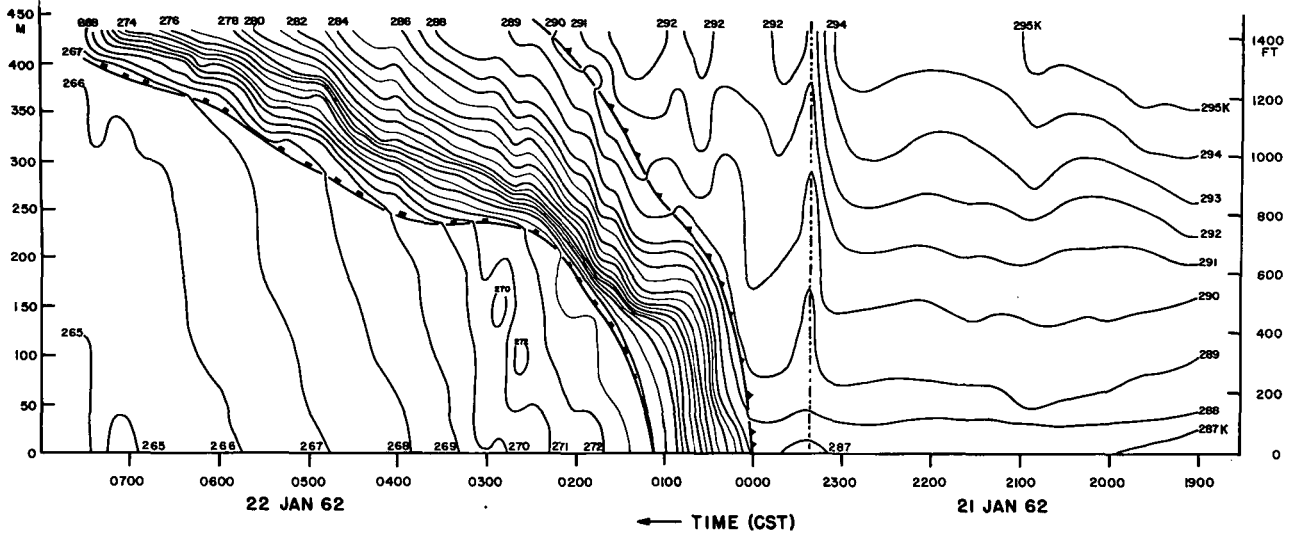


FIGURE 15.—The time cross section of potential temperature at the tower for Case 9, January 22, 1962. The slightly heavier lines represent the boundaries of the frontal zone. The vertical dash-dot line shows the position of a squall line which preceded the front. (After Shimomura.)

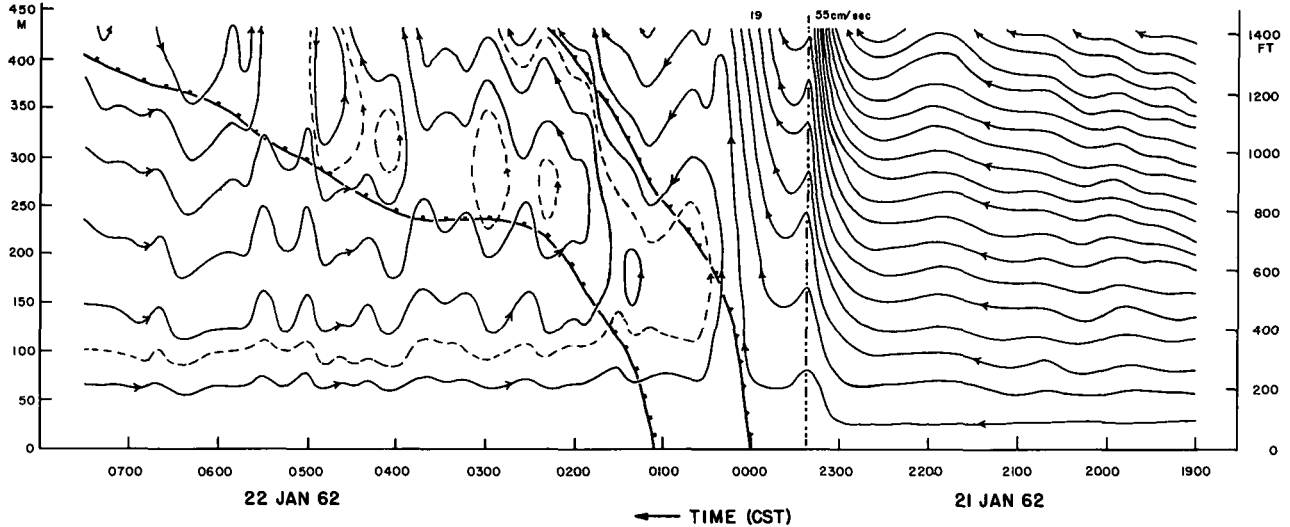


FIGURE 16.—The relative streamlines for Case 9 based on the motion of the front. Values of w (cm.sec.⁻¹) are shown at the top of the figure in regions of strong vertical motion. (After Shimomura.)

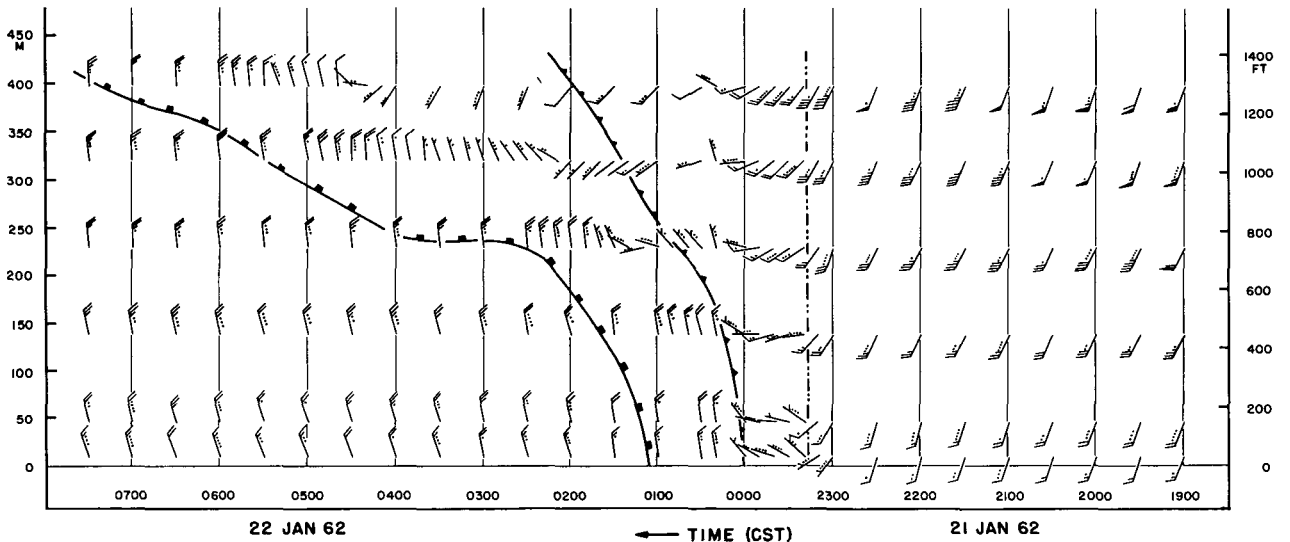


FIGURE 17.—The wind field for Case 9 at selected times and levels of the tower. The arrows are oriented with north at the top of the figure and speeds are in mi.hr.⁻¹. The wind barbs have their standard meaning except that dots have been used for 1 mi.hr.⁻¹. (After Shimomura.)

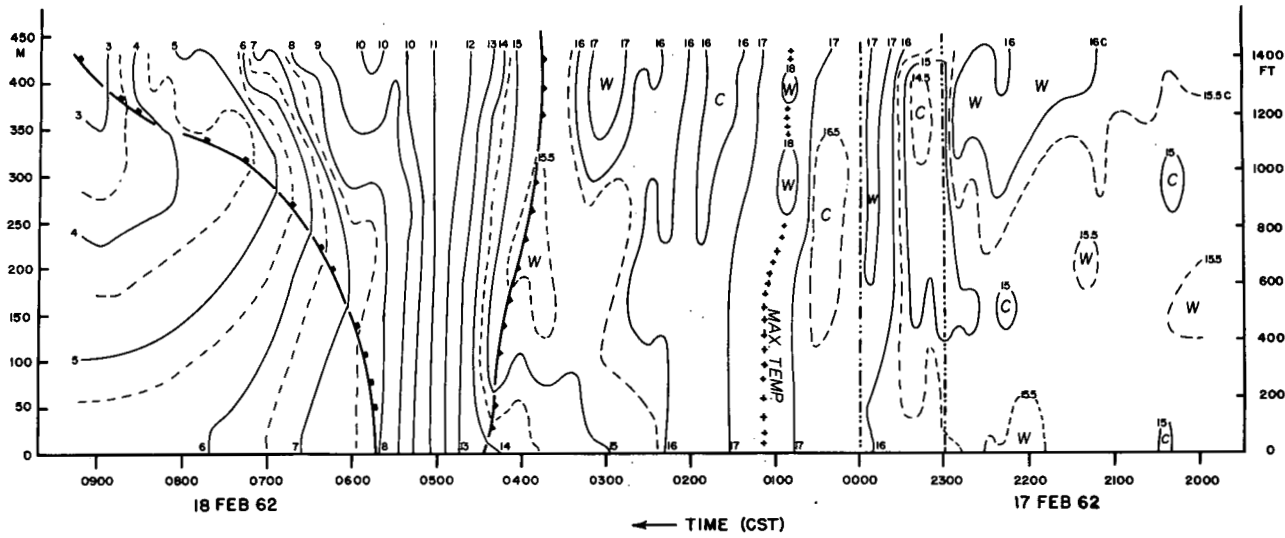


FIGURE 18.—The time cross section of temperature ($^{\circ}\text{C}$) at the tower for Case 10, February 18, 1962. See legend for figure 15. (After Shimomura.)

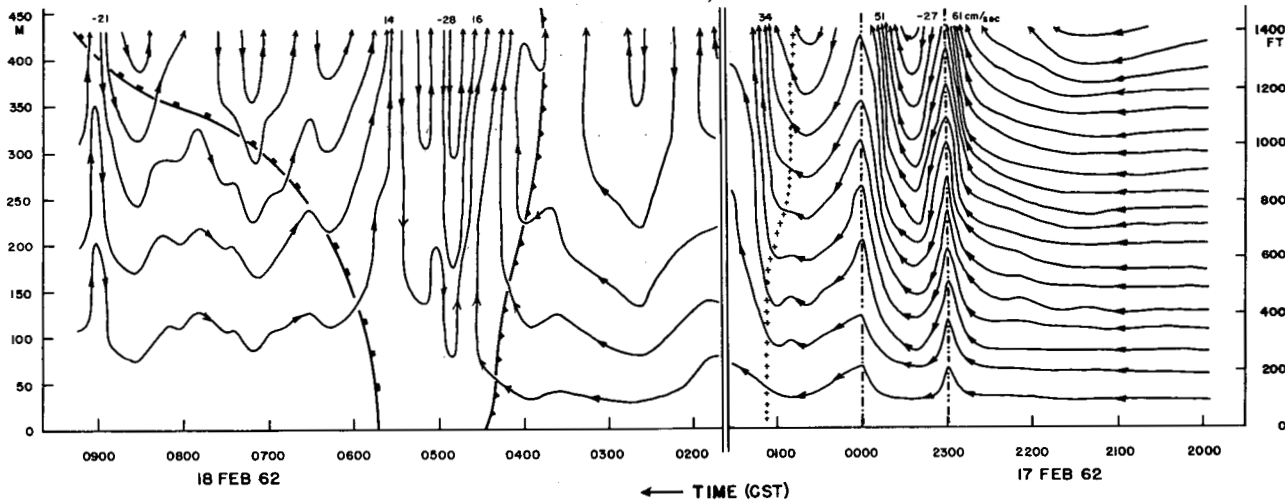


FIGURE 19.—The ψ field for Case 10. Streamlines to the left of the break at 0140 cst are based on the motion of the front, those to the right of the break are based on the motion of the squall line. Values of w ($\text{cm}\cdot\text{sec}^{-1}$) are shown along the top for regions of significant vertical motion. (After Shimomura.)

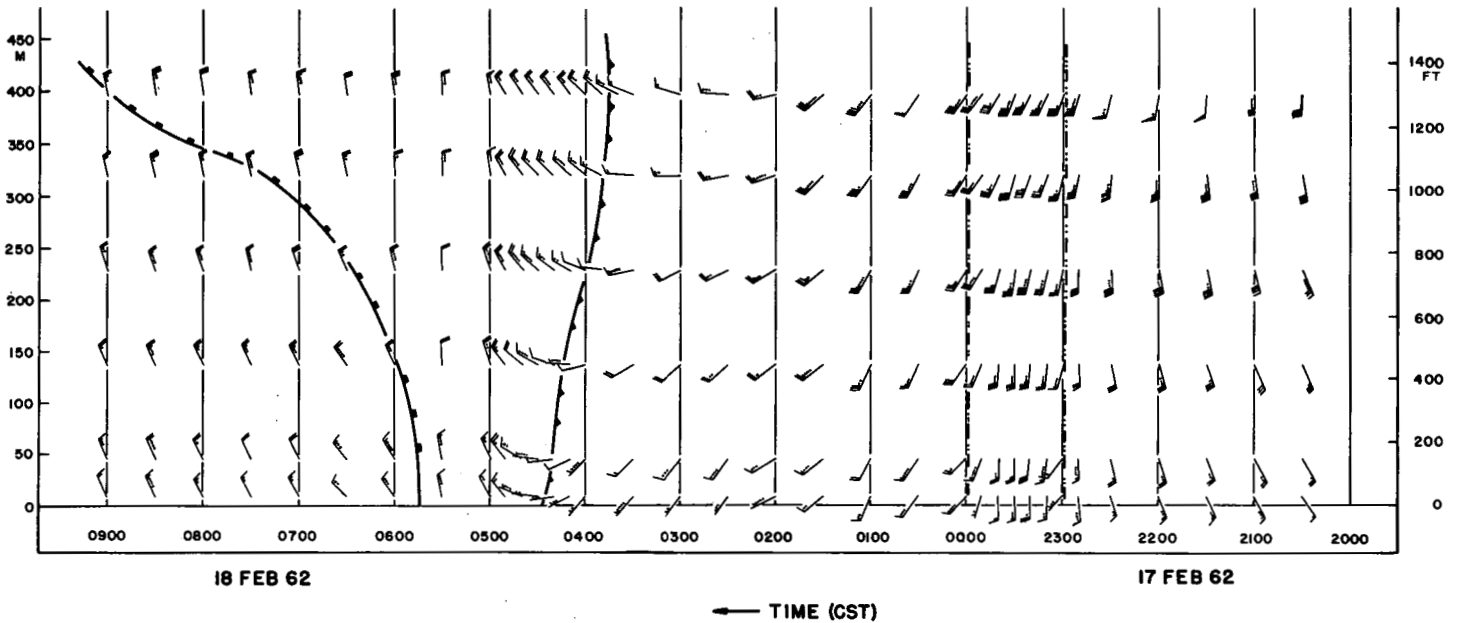


FIGURE 20.—The wind field for Case 10. See legend for figure 17. (After Shimomura.)

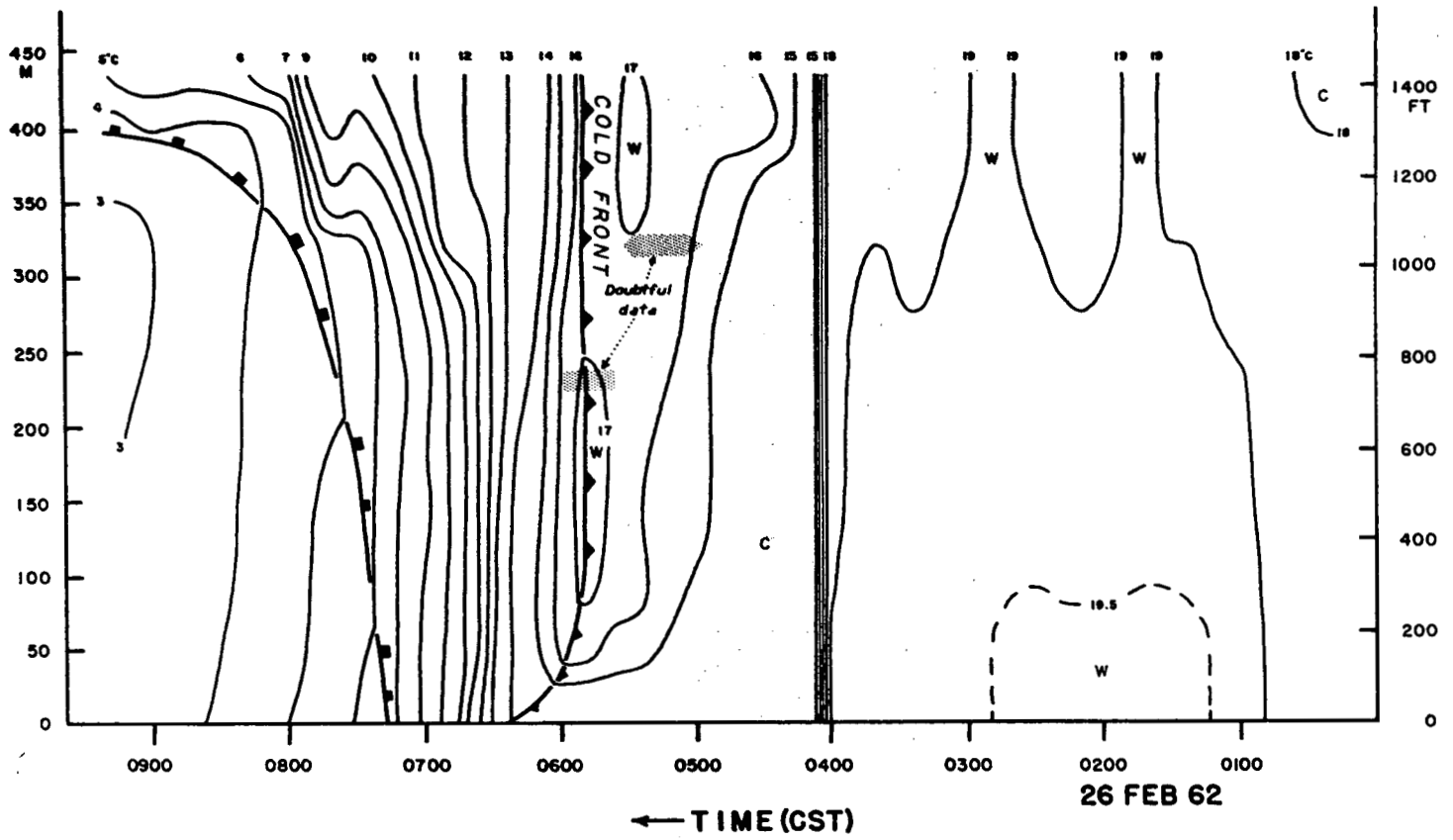


FIGURE 21.—The temperature field (°C.) measured at the tower for Case 11, February 26, 1962. The squall line is indicated by the concentration of isotherms which preceded the Arctic front by about 2 hr. (After Shimomura.)

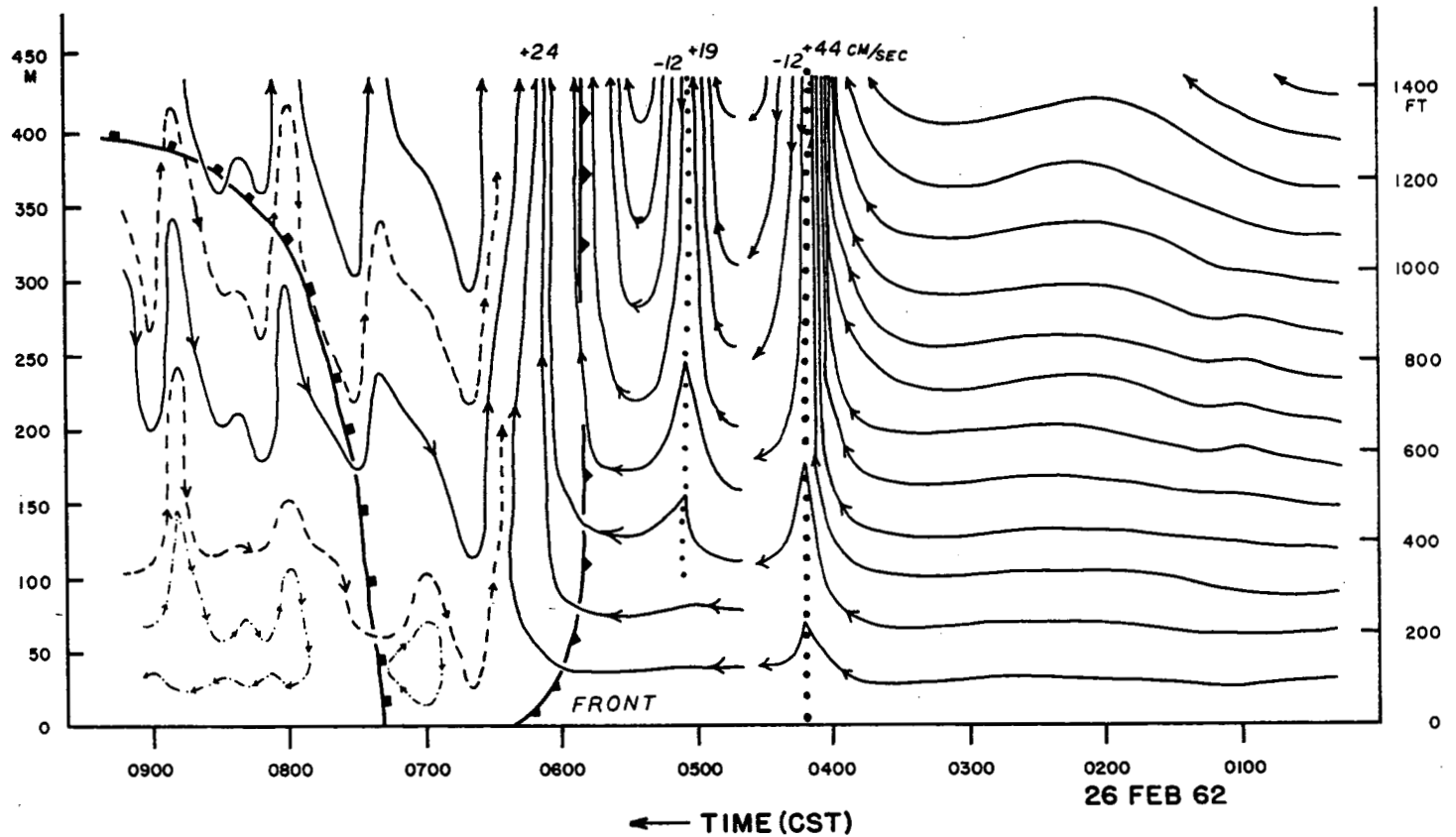


FIGURE 22.—The relative streamlines for Case 11. Streamlines after the break at 0440 CST are based on the motion of the front, whereas those prior to the break are based on the motion of the squall line. (After Shimomura.)

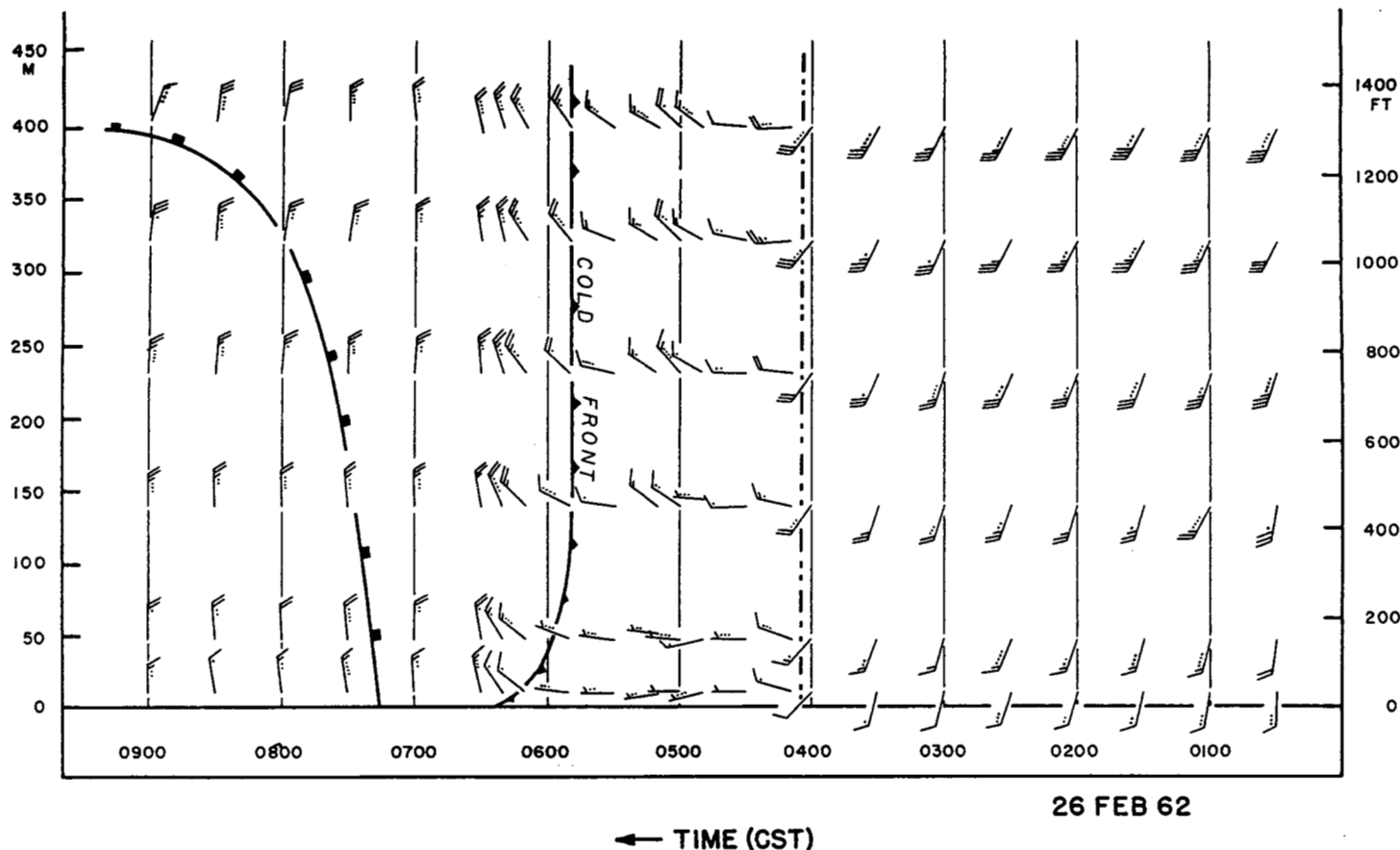


FIGURE 23.—The wind field for Case 11. See legend for figure 17. (After Shimomura.)

top of the figures for orientation and the barbs have their usual meaning. Dots represent 1 mi. hr.^{-1} . The figures show that in each case the squall line was located on the western flank of a low-level wind maximum with speeds in excess of 40 mi. hr.^{-1} appearing at the upper levels of the tower. They also show, as stated before, that the line of $v=0$ falls behind the frontal surface, particularly in the upper levels away from the strong surface frictional influences. This condition would appear to support Godson's [6] suggestion that the trough in the pressure field should occur behind the frontal surface.

5. TOWER AND RAWIN WINDS

In order to carry out the computations of the various kinematic fields, it has been necessary to assume that the wind field is essentially steady-state in a coordinate system moving with the front. The validity of this assumption is difficult to ascertain.

For the present group of cases the only comparison that could be made was between the tower winds and rawin measurements at ACF. It could not be expected that very exact agreement would be found because of the differences in instruments and measuring techniques that were involved, and also because the measurements generally were in different vertical planes normal to the front. Another problem was that ACF is at 575 ft. MSL whereas

the tower site is at 825 ft. above sea level. It was decided to make the comparison between measurements at about the same relative heights above the ground. Accordingly, the ACF winds at the surface, 1,000 ft. MSL, and 2,000 ft. MSL were compared with the 30-ft., 450-ft., and 1,300-ft. winds, respectively, at the tower. The 1,420-ft. tower wind should have been used in this comparison rather than the 1,300-ft. value; however, there was some shielding of the instrument at this level by the tower framework for winds out of the northwest quadrant which made its values consistently too low. The results, in terms of $u-c$, for the first eight cases are summarized in table 3.

In order to arrive at the values in table 3, it was necessary to project ACF onto the vertical plane passing through the tower and normal to the front. The resulting distance between the projection of ACF and the tower was then converted into travel time in order to determine the equivalent time of the rawin in the tower time cross section. These times constitute the second line of the table. In Cases 1 and 4, computations of tower values had not been performed at times corresponding to the 1200 GMT rawin. In Cases 9 and 10, the computations for the tower data were not available to the writer; however, the sign of the relative motion could be determined from figures 16 and 19.

On the whole the agreement is quite good, although

Table 3.—Comparison of values of $u-c$ (m. sec.⁻¹) from tower and ACF rawin measurements

Case	1		2		3		4		5		6		8	9		10	
	0600	1200	0600	1200	0600	1200	0600	1200	0600	1200	0000	0600	0000	0600	1200	1200	
Rawin time (GMT)																	
Corresponding tower time (CST)	0049	0649	0040	0640	0100	0700	0100	0700	0200	0800	1830	0030	1830	0117	0717	0700	
Grd.-----	ACF -----	≈0	-4.1	-5.2	-5.0	-10.3	-1.0	-5.0	4.6	-4.0	1.0	-4.6	-9.3	-3.1	3.6	3.6	-3.1
	Tower -----	-2.5	Msg. -6.7	-6.6	-9.4	-0.6	-3.0	Msg. -1.7	2.0	-10.6	-9.4	-4.1	+	+	+	+	
450 ft.-----	ACF -----	1.3	-1.7	-6.0	-6.6	-11.9	1.0	-5.6	3.1	-2.8	2.8	-4.6	-3.9	-1.0	2.3	9.3	1.8
	Tower -----	1.0	Msg. -13.0	-10.4	-7.6	1.3	-7.2	Msg. 1.0	4.0	-5.8	-3.9	2.8	+	+	+	+	
1,300 ft.-----	ACF -----	-3.0	-1.7	-11.0	-6.0	-7.6	-4.5	-7.2	3.1	0	2.8	1.0	3.1	0.5	-6.2	2.8	3.1
	Tower -----	-3.0	Msg. -11.7	-7.3	-9.0	-4.3	-8.0	Msg. 3.5	6.0	-5.0	3.4	3.5	-	+	+	+	

there are several instances of a sign discrepancy and/or a large difference in magnitude. The time increments range from 30 min. to 2 hr. It would therefore appear, that while the procedure used undoubtedly leads to some error in the computed values of divergence and vertical motion, the essential features are probably correct.

On the basis of wind shifts, the 0600 GMT rawins at ACF for Cases 1, 3, and 4 also indicated that the frontal surface departs abruptly from its near-vertical shape to bend back over the colder air somewhere between 2,000 and 3,000 ft.

6. COMPARISONS AND COMMENTS

The relative streamline patterns given here are found to be in general agreement with those appearing in Clarke's [2] work, if one's attention is confined to below 500 m. in his figures.

While considerably less detail appears at these levels in Clarke's streamline patterns, there is the same tendency for confluence of warm and cold currents in the frontal zone with cross-isentropic motion, and occasionally some horizontal vortices in the cold air. It is not clear from Clarke's figures whether or not he found the same penetration of warm air into the cold air mass at the lowest levels but presumably this would be the case. Only one of his cold front cases (fig. 11d) and several of his sea breeze fronts show the deep warm-air penetration at all levels below 500 m., such as found in Cases 2 and 7.

Above 500 m. Clarke's streamline patterns show anafont flow [13] in every case, i.e., relative motion of the warm air up the frontal boundary. In the present study, the rawin reports at ACF indicate that Cases 1, 2, 3, 4, and 9 are anafronts, whereas Cases 5, 6, 8, and 10 are katafronts. The situation for Cases 7 and 11 could not be determined because of missing data for ACF.

Sanders' [12] case study also shows many features similar to those found here. Sanders also found evidence that the warm boundary of the frontal zone could not be considered a substantial surface, that warm air was being incorporated into the frontal zone during its southward movement. He states that the front moved with the normal component of the cold air and thus entrainment of cold air through the cold boundary was not indicated. However, his figure 18, which shows a plot of u versus c for the surface wind at

points 1 hr. behind the front, has twice as many points of $u-c > 0$ as points of $u-c < 0$. Only four points indicate $u-c = 0$. This would seem to imply the possibility of some cold-air entrainment; however, it should be noted that the relative streamlines given in the present study indicate that generally $u-c < 0$ near the ground behind the front. The cold-air entraining current is higher up.

As in the present study, Sanders found the leading portion of the frontal zone has a motion toward the low-pressure center. That is, the line $v=0$ lies just behind the warm boundary of the frontal zone at the ground and falls farther back with height. For the cases given here, the distance of the line $v=0$ behind the front at 30 ft. ranged from 0 to 8.5 mi. with an average of 2.8 mi. At the top of the tower, the range was from 8 to 42 mi. with an average of 25 mi.

Finally, Sanders computed values of horizontal convergence and upward motion in the frontal zone at 1,000 ft. comparable in magnitude to those found in this study (table 2). Sanders' figure 10 indicates that the values of w attain a maximum above the frontal zone in the vicinity of the 850-mb. surface. From the values given in table 2 this implies that in many instances very large values of w should be encountered at this level unless a compensating change in the sign of the divergence occurs above the frontal zone. Clarke's figures indicate the same situation. It is in this region that Newton [10] has hypothesized that squall lines may form.

Newton [11] has discussed frontogenetic and frontolytic processes in the middle troposphere from the point of view of the changes of temperature gradient and wind-shear experienced by individual fluid parcels as they enter a frontal zone from the west and depart to the east. Sanders [12] performs a similar analysis to explain what must happen to a parcel of air passing from the warm-air mass into the frontal zone, and hence to higher levels in the frontal zone. His frontogenetic function for the temperature field expressed in the coordinate system used here becomes

$$\frac{d}{dt} \left(\frac{\partial \theta}{\partial x} \right) = \frac{\partial}{\partial x} \left(\frac{d\theta}{dt} \right) - \left(\frac{\partial u}{\partial x} \frac{\partial \theta}{\partial x} + \frac{\partial w}{\partial x} \frac{\partial \theta}{\partial z} \right) \quad (5)$$

He neglected the first term on the right. It seems very likely that had a similar analysis been performed for the

cases examined here, the results would have been quite close to those given by Sanders in his figures 13 and 17. These figures show strong frontogenetic influences in the warm air and within the frontal zone below about 950 mb. The pressure at the top of the Dallas tower ranged from about 940 to 960 mb., depending upon the surface pressure, for the cases shown here.

The magnitudes which Sanders computed appear to be great enough to account for the incorporation into the frontal zone of parcels from the warm-air mass. However, if the relative streamlines shown here and in Clarke's work are at all representative of the relative trajectories of the fluid parcels then, frequently, cold air also enters the frontal zone and must undergo frontogenesis. Sanders' computations would not appear to provide a sufficient degree of individual frontogenesis in this region. It would seem that in this region, as well as within the frontal zone itself, the first term on the right of equation (5) would be of some importance because of turbulent mixing, as was indeed recognized by Sanders.

Sanders also suggests that the near-adiabatic lapse rate generally found in the cold air behind fronts is probably a result of warming of the air by the ground. However, the present study shows that there is actually a shallow layer of air at the ground which is left behind by the front and which must cool as it contributes through vertical turbulent mixing to the warming of the upper cold current.

Even aside from the question of the possible importance of the first term on the right of equation (5), there is also the question of whether individual frontogenesis or frontolysis is representative of local changes of gradient. Upon expanding the left-hand side of equation (5) and rearranging terms, one obtains

$$\frac{\partial}{\partial t} \left(\frac{\partial \theta}{\partial x} \right) = \frac{\partial}{\partial x} \left(\frac{d\theta}{dt} \right) - \frac{\partial C}{\partial x} \cdot \nabla \theta - C \cdot \nabla \frac{\partial \theta}{\partial x} \quad (6)$$

Again ignoring the first term on the right, it is seen that at a given point the individual frontogenetic function could be positive, yet the local gradient could be decreasing with time. As an example, if u were negative in the warm air just ahead of the front, there would be a contribution to local frontolysis from the third term on the right of equation (6). The same term would contribute to frontogenesis in the cold air if u were negative. If this situation persisted for some time and was dominant, it could lead to an eventual apparent retrogression of the front. This might explain some of the behavior of the temperature field in Case 2.

However, once a frontal zone is established in the temperature and wind fields, it would seem more reasonable to examine its changes within the framework of a coordinate system moving at the speed, c , of the front. The change in $\partial\theta/\partial x$ at a point fixed in the moving coordinate system is

$$\frac{D}{Dt} \left(\frac{\partial \theta}{\partial x} \right) = \frac{\partial}{\partial x} \left(\frac{d\theta}{dt} \right) - \frac{\partial C}{\partial x} \cdot \nabla \theta - C' \cdot \nabla \frac{\partial \theta}{\partial x}, \quad (7)$$

where $C' = i(u-c) + \hat{k}w$.

If turbulent mixing is the primary consideration in its evaluation, the first term on the right of equation (7) should contribute negatively within a frontal zone. From Sanders' calculations, the second term will generally be a large positive value. Somewhere within the frontal zone there should lie a surface of maximum $\partial\theta/\partial x$. From the relative motion found in this study, the third term on the right side of equation (7) would probably contribute negatively on either side of this surface of maximum horizontal temperature gradient, except in the region of warm-air influx near the ground behind the front, and other places in the cold air where the relative motion is from warm to cold. Thus, there is the possibility that the three terms on the right side of equation (7) could very nearly balance, i.e., the front would move along relatively unchanged even though individual frontogenesis is indicated. If it could be definitely established that the temperature field is steady-state or, at least, that the left-hand side of equation (7) is negligibly small, the first term on the right could be solved for and some estimates could be made of the turbulent heat exchange process in frontal zones. Some work along these lines has been carried out by Clarke [2] and Conlan [1].

7. SUMMARY

This study reveals that the temperature structure in frontal zones near the ground at night may be quite complicated but approaches the textbook case with increasing baroclinity. The overrunning cold front apparently is a very common phenomenon at night when the abutment of frontal zone and nocturnal inversion provides a stable situation.

The relative flow patterns generally show a confluence of warm-air and cold-air currents within the frontal zone, indicating that the frontal surface cannot be treated as a substantial surface. The penetration of the warm-air current is greater near the ground, evidently as a result of frictional influences. A comparison of the tower data with rawin data indicates that the relative flow is quite conservative, at least for periods up to an hour. This comparison could be turned around to imply that rawin observations provide an adequate means to determine the gross features of the horizontal portion of the relative flow when used within an hour of release time.

While the conversion of a time section into a space section is an equivocal procedure it seems reasonable to expect that local changes in a moving frontal zone would be relatively small over a period of several hours. Thus, it would seem that the results given here are fairly representative of conditions which may be found in fronts during fall and winter nights.

ACKNOWLEDGMENTS

The author wishes to thank Mr. E. Y. J. Wong who performed some of the analyses and Mr. D. S. Shimomura who wrote the IBM 709 program to carry out the computations. Thanks are also extended to Mr. Shimomura for the use of some of his figures. Finally, grateful acknowledgment must be given to the Air Force Cambridge Research Laboratories for their support of this work under Contract AF 19(604)-7455.

REFERENCES

1. K. C. Brundidge, H. Beniura, E. Y. J. Wong, B. C. Ryan, and E. F. Conlan, "Mesoscale Circulations of the Atmospheric Boundary Layer," *Final Report*, Contract AF 19(604)-7455, Texas A & M University, 364 pp.
2. R. H. Clarke, "Mesoscale Structure of Dry Cold Fronts over Featureless Terrain," *Journal of Meteorology*, vol. 18, No. 6, Dec. 1961, pp. 715-735.
3. W. H. Clayton, "An Automatic Micrometeorological Data-Collection Station," *Final Report*, Contract AF 19(604)-6200, Texas A & M University, 127 pp.
4. J. R. Gerhardt, "An Example of a Nocturnal Low Level Jet Stream," *Journal of the Atmospheric Sciences*, vol. 19, No. 1, Jan. 1962, pp. 116-118.
5. J. R. Gerhardt, "Mesoscale Association of a Low-Level Jet Stream with a Squall-Line—Cold-Front Situation," *Journal of Applied Meteorology*, vol. 2, No. 1, Feb. 1963, pp. 49-55.
6. W. L. Godson, "Synoptic Properties of Frontal Surfaces," *Quarterly Journal of the Royal Meteorological Society*, vol. 77, No. 334, Oct. 1951, pp. 633-653.
7. Y. Izumi and M. L. Barad, "Wind and Temperature Variations during Development of a Low-Level Jet," *Journal of Applied Meteorology*, vol. 2, No. 5, Oct. 1963, pp. 668-673.
8. Y. Izumi, "The Evolution of Temperature and Velocity Profiles during Breakdown of a Nocturnal Inversion and a Low-Level Jet," *Journal of Applied Meteorology*, vol. 3, No. 1, Feb. 1964, pp. 70-82.
9. W. S. Mitchem and K. H. Jehn, "Operation and Performance of the Cedar Hill Meteorological Tower Facility," *Final Report*, Contract AF 19(628)-2459, The University of Texas, 43 pp.
10. C. W. Newton, "Structure and Mechanism of the Prefrontal Squall Line," *Journal of Meteorology*, vol. 7, No. 3, June 1950, pp. 210-222.
11. C. W. Newton, "Frontogenesis and Frontolysis as a Three-Dimensional Process," *Journal of Meteorology*, vol. 11, No. 6, Dec. 1954, pp. 449-461.
12. F. Sanders, "An Investigation of the Structure and Dynamics of an Intense Surface Frontal Zone," *Journal of Meteorology*, vol. 12, No. 6, Dec. 1955, pp. 542-552.
13. H. W. Sansom, "A Study of Cold Fronts over the British Isles," *Quarterly Journal of the Royal Meteorological Society*, vol. 77, No. 331, Jan. 1951, pp. 96-120.
14. W. J. Saucier, *Principles of Meteorological Analysis*, The University of Chicago Press, Chicago, 1955, 438 pp.
15. D. W. Stevens and J. R. Gerhardt, "A New Meteorological Research Tower," *Bulletin of the American Meteorological Society*, vol. 40, No. 1, Jan. 1959, pp. 24-26.
16. R. H. Thuillier and U. O. Lappe, "Wind and Temperature Profile Characteristics from Observations on a 1400 Ft. Tower," *Journal of Applied Meteorology*, vol. 3, No. 3, June 1964, pp. 299-306.
17. S. S. Wu, "A Study of Heat Transfer Coefficients in the Lowest 400 Meters of the Atmosphere," *Journal of Geophysical Research*, vol. 70, No. 8, pp. 1801-1807.

[Received May 28, 1965; revised August 12, 1965]